

Enhancing High-Order Above-Threshold Dissociation of H_2^+ Beams with Few-Cycle Laser Pulses

J. McKenna, A. M. Saylor, F. Anis, B. Gaire, Nora G. Johnson, E. Parke, J. J. Hua, H. Mashiko, C. M. Nakamura, E. Moon, Z. Chang, K. D. Carnes, B. D. Esry, and I. Ben-Itzhak

J. R. Macdonald Laboratory, Kansas State University, Manhattan, Kansas 66506, USA

(Received 30 July 2007; published 1 April 2008)

High-order (three-photon or more) above-threshold dissociation (ATD) of H_2^+ has generally not been observed using 800 nm light. We demonstrate a strong enhancement of its probability using intense 7 fs laser pulses interacting with beams of H_2^+ , HD^+ , and D_2^+ ions. The mechanism invokes a dynamic control of the dissociation pathway. These measurements are supported by theory that additionally reveals, for the first time, an unexpectedly large contribution to ATD from highly excited electronic states.

DOI: [10.1103/PhysRevLett.100.133001](https://doi.org/10.1103/PhysRevLett.100.133001)

PACS numbers: 33.80.Wz, 42.50.Hz

The importance of a firm knowledge of how molecules respond to an intense laser field is highlighted by the plethora of possible applications reliant on this information. These applications include molecular alignment [1], molecular structural deformation [2], high-harmonic generation [3], femtochemistry [4], and adaptive control experiments [5], to name only a few. Despite intensive research in this field over many years, the complicated multiphoton dynamics of a molecule in a laser field continues to unveil fresh surprises as evidenced recently by the new structure resolved in the laser-induced ionization of H_2^+ molecules [6,7].

Since the discovery of above-threshold ionization of atoms [8], the molecular analogue—above-threshold dissociation (ATD)—has been widely anticipated [9,10]. In this process, more photons than the minimum number needed to dissociate are absorbed. In the case of H_2^+ where the minimum number is one, absorption of two or more photons qualifies for ATD, and, for convenience, should three or more be absorbed we will refer to the process as “high-order.” Strangely, in spite of early experimental evidence for high-order ATD of H_2^+ at 532 and 1064 nm wavelengths [11–13], detection using 800 nm light has proven difficult. Against this trend, an observation of high-order ATD has very recently been reported using a vibrationally cold target of HD^+ [14].

Detailed inspection using the Floquet representation for the light-dressed states (e.g., Ref. [15]) of H_2^+ reveals why high-order ATD is normally obscure. Figure 1(a) shows the diabatic $1s\sigma_g$ and $2p\sigma_u$ Born-Oppenheimer potentials, shifted in energy by the number of absorbed photons. Both of these states converge to the $\text{H}^+ + \text{H}(1s)$ atomic limit. For laser intensity $\geq 10^{12}$ W/cm², the adiabatic potentials—which include the effects of the laser-molecule coupling—are more appropriate. The resulting adiabatic pathways for dissociation are indicated in the figure with arrows. Whether the molecule follows these adiabatic pathways or more diabatic ones depends on the intensity of the laser pulse when the dissociating wave packet passes through the crossing. For example, at low intensity

($\sim 10^{12}$ W/cm²) dissociation is dominated by one-photon absorption, depleting the population of high vibrational states, $v \sim 9$. At higher intensity, the three-photon crossing $|1s\sigma_g - 0\omega\rangle \rightarrow |2p\sigma_u - 3\omega\rangle$ opens, with population from the low- v states dissociating. This population tends to end up in the *net* two-photon channel ($1s\sigma_g - 2\omega$) via reemission of a photon at the second crossing encountered along this pathway. For the same reasons, the observation of net three-photon ATD ($2p\sigma_u - 3\omega$) requires an initial absorption of five photons, net four-photon ATD requires absorption of seven photons, and so on. The fact that dissociation follows the adiabatic pathway makes observation of high-order ATD difficult.

In this Letter we explore, through theory and experiment, the possibility of blocking the paths that lead back to low-order ATD via channel closing, thereby enhancing the high-order processes. We do so using laser pulses that are intense enough to open the first ATD crossing with the ground state, but also short enough to “switch off” before the dissociating H_2^+ wave packet can reach the later curve

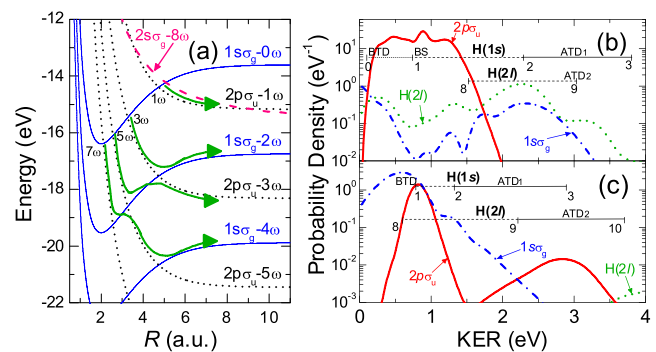


FIG. 1 (color online). (a) Field-free Born-Oppenheimer potentials of H_2^+ , dressed by net absorbed number of photons, $n\omega$. (b) Dissociation probability of the $v = 9$ H_2^+ level (10 fs, 1×10^{14} W/cm² pulse) showing final population contributions for the $\text{H}(1s)$ $1s\sigma_g$ and $2p\sigma_u$, and $\text{H}(2l)$ electronic states. (c) Same as (b) for $v = 3$. Tick marks with labels denote net photons absorbed (BTD \equiv below-threshold dissociation), indicating diabatic energy release from initial v state to $E(R = \infty)$.

crossings along its path. By this combination we can control the dissociation path of the molecule, forcing it into high-order ATD channels. We also identify a new ATD mechanism: excitation to the $H(2l)$ states of H_2^+ accompanied by the absorption of an excess number of photons. All previous interpretations of ATD have been based only on $H(1s)$ states.

As the least massive molecule, H_2^+ is the fastest to evolve temporally. For example, its $v = 0$ vibrational period is 14 fs, and we estimate classically the typical travel time between consecutive crossings to be only a few femtoseconds. Manipulating the dissociation path, therefore, requires laser pulses even shorter than this. The 7 fs laser pulses we use here would seem inadequate for the task, but by contrasting H_2^+ with the more massive HD^+ and D_2^+ , and thus varying the effective time scales, one can make the high-order ATD contributions more evident.

Figures 1(b) and 1(c) show the dissociation probability of the $v = 9$ and $v = 3$ states, respectively, of H_2^+ from our time-dependent calculations. These states exemplify precisely the difficulties involved in observing high-order ATD from $H(1s)$ (hereafter referred to as ATD_1)—that is, the almost negligible probability for mechanisms requiring more than net two-photon absorption. To identify the different mechanisms in the figures, we note that for ATD_1 , net absorption of an even number of photons leads to dissociation on $1s\sigma_g$, and net absorption of an odd number, to dissociation on $2p\sigma_u$. The tick marks may be used as a guide to the expected positions of the resulting peaks, showing also the contributions from $H(2l)$. For $v = 9$, one-photon dissociation dominates as $v = 9$ is near resonance with the 1ω crossing. For low vibrational states, where contributions to high-order ATD are anticipated to be largest (e.g., $v = 3$, resonant with the 3ω crossing), the three-photon probability is still more than 2 orders of magnitude below the one- and two-photon probabilities. Such a rapid decrease in probability for high-order ATD is evident in the early experimental work of Bucksbaum *et al.* [11] on H_2 at 532 nm.

Figure 1 also shows that the high vibrational states, for example $v = 9$, display a strong contribution to ATD from $H(2l)$ states (ATD_2) showing multiple peaks from the absorption of excess photons. As the $H(2l)$ states lie many photon energies above the $H(1s)$ manifold, such excitations are normally neglected in literature. However, as illustrated in the theoretical work of Nguyen–Dang *et al.* [16], their involvement can be important, and indeed is necessary, to explain observations of perpendicular transitions [17,18] at 400 nm. In addition, Gibson *et al.* [19] recently reported a direct measurement of net eight-photon excitation of the $H_2^+ 2s\sigma_g$ state using 800 nm light. Our results show that, in addition to the inclusion of excitation to the $H(2l)$ manifold being essential, the $H(2l)$ states can dissociate above their threshold, i.e., by absorbing nine photons with non-negligible probability as opposed to the

minimum number of eight. In particular, the probability of ATD_2 is found to outweigh that of high-order ATD_1 , further emphasizing the suppressed nature of the latter.

In our theoretical approach [20], we solved the time-dependent Schrödinger equation in the Born-Oppenheimer representation, including nuclear rotation, nuclear vibration, and electronic excitation, but neglecting the Coriolis and all nonadiabatic couplings. As ionization is omitted from the theory, we limit the intensities explored to below the ionization threshold. This theoretical approach is a generalization of our previous formulation for aligned molecules which we solve using a similar numerical scheme [21]. Figures 2(a) and 2(b) show Franck-Condon averaged (weighted average over all v states) dissociation probabilities for a 7 fs pulse, as a function of kinetic energy release (KER) and $\cos\theta$, where θ is the angle between the molecular bond axis and the laser polarization. To obtain these distributions, we superposed the scattering solutions for each electronic channel to obtain a solution that asymptotically behaved as an outgoing plane wave [22]. The projection of the total time-dependent wave function after the pulse on this scattering solution gives the KER- $\cos\theta$ distribution.

At 2×10^{13} W/cm² [Fig. 2(a)], dissociation is almost exclusively due to one-photon absorption. The angular distribution is characteristic of bond softening (BS) [9–11] as illustrated previously for longer pulses (e.g., Ref. [21]). However, increasing the intensity to 10^{14} W/cm²

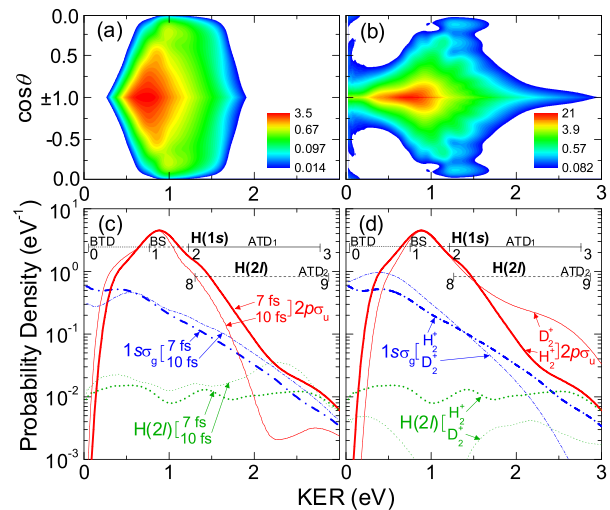


FIG. 2 (color online). (a) Calculated KER- $\cos\theta$ probability density (in units of $10^2 \cos\theta^{-1} \text{ eV}^{-1}$) maps for H_2^+ using 7 fs 2×10^{13} W/cm² pulses. (b) Same as (a) for 10^{14} W/cm². (c) Dissociation probability density at 10^{14} W/cm² for a 7 and 10 fs pulse showing $1s\sigma_g$, $2p\sigma_u$, and $H(2l)$ contributions with the peak value of their sum normalized. (d) Same as (c) for 7 fs H_2^+ and D_2^+ comparison. All probability densities are Franck-Condon averaged over all v states. Ticks with labels denote net photons absorbed, indicating diabatic energy release from curve crossings with the ground state to $E(R = \infty)$.

[Fig. 2(b)] leads to several changes. First, the overall spectrum becomes much narrower in angle. This is consistent with the fact that ATD requires a high effective field along the molecular axis to drive high-order parallel ($\sigma \rightarrow \sigma$) transitions. Hence, by geometric alignment, ATD will preferentially dissociate those molecules aligned with the field. Second, the spectrum develops a striking high-KER tail. To understand this tail, Fig. 2(c) shows a decomposition of this spectrum into the individual state contributions, revealing that while one-photon absorption is still the dominant channel, the tail is a mixture of ATD₁ and ATD₂ processes via *three* and *nine* photon transitions, respectively (see tick marks). Note, the latter is more than the minimum required to dissociate to $H^+ + H(2l)$.

Comparison to a 10 fs pulse [Fig. 2(c)] shows that the three-photon 7 fs probability ($2p\sigma_u$ KER ~ 2.5 eV) is enhanced by almost an order of magnitude. Simultaneously, the two-photon probability ($1s\sigma_g$ KER ~ 1.8 eV) drops, suggesting that flux is being channeled from one process to the other—exactly the result sought to show closing of the $|1s\sigma_g - 2\omega\rangle \rightarrow |2p\sigma_u - 3\omega\rangle$ crossing. An additional order of magnitude enhancement in the three-photon probability is achievable by replacing H_2^+ with D_2^+ [Fig. 2(d)]. This isotopic dependence is caused by the more massive D_2^+ nuclear wave packet taking longer to reach the $|1s\sigma_g - 2\omega\rangle \rightarrow |2p\sigma_u - 3\omega\rangle$ crossing. Thus, rather than following the adiabatic 2ω pathway, channel closing diverts it into the 3ω channel. Interestingly, Figs. 2(c) and 2(d) show that ATD₂ follows the reverse trend to the high-order ATD₁ enhancement, getting suppressed for D_2^+ and shorter pulses. This would suggest that ATD₂ is similarly affected by channel closing. A Floquet picture incorporating the $H(2l)$ states, as illustrated for $|2s\sigma_g - 8\omega\rangle$ in Fig. 1(a), shows that the excited states may indeed cross the dissociative $|2p\sigma_u - 1\omega\rangle$ curve at larger R , e.g., $|1s\sigma_g - 0\omega\rangle \rightarrow |2p\sigma_u - 1\omega\rangle \rightarrow |2s\sigma_g - 8\omega\rangle$. As the second step of such a sequence is time delayed with respect to the first, the use of short pulses will, therefore, suppress the $H(2l)$ excitation step. Our calculations indicate the largest suppression is for the $2s\sigma_g$ and $3p\sigma_u$ states.

Using the high-KER fragments of dissociation as a clear signature of the high-order ATD processes, we will now test these theoretical predictions experimentally.

In the experiments we used a molecular hydrogen ion beam target (see, e.g., [23–25]). This eliminated all possibility of electron recollision dissociation which is known to overlap in KER with the ATD processes [26]. In addition, since the molecular ions were formed in an isolated source, their dissociation could be probed at low laser intensity, which is more amenable to our theory. To clearly separate the dissociation and ionization events, a coincidence 3D momentum imaging method [25] was employed. The laser was a Ti:sapphire (800 nm) system providing linearly polarized 7 fs (FWHM) pulses compressed using a neon-filled hollow-core fiber and chirped mirror arrange-

ment [27]. These pulses were focussed on target using an $f = 203$ mm off-axis parabolic mirror, with the intensity varied using an intensity selective scan method [28]. Our target consisted of a beam of either H_2^+ , HD^+ , or D_2^+ ions formed in an electron-impact ion source and accelerated to 9.0 keV. Following laser fragmentation, a small electrostatic field in the interaction region applied along the molecular beam axis was used to temporally separate the charged products from the neutrals. This allowed a coincidence measurement of atom-ion and ion-ion events thus clearly distinguishing dissociation from ionization. The fragments were detected using a 2D microchannel plate delay-line detector operating in event mode. The primary beam was collected in a small on-axis Faraday cup that prevented detection of dissociation events with KER < 0.02 eV. From the position and time information recorded for both fragments, the complete 3D kinematics of the breakup events were computed.

Figures 3(a)–3(d) show the measured dissociation spectra of H_2^+ and D_2^+ for both low, 2.0×10^{13} W/cm², and high, 2.5×10^{15} W/cm², intensities. The higher intensity does not match that given in Fig. 2(b) since the theory was limited to intensities below the onset of ionization ($\sim 2 \times 10^{14}$ W/cm²). However, experimentally the goal was to magnify the effects of ATD which are more apparent at high intensity, despite some ionization ($\sim 14\%$) that will deplete, particularly, the higher-order ATD channels. In addition, as a general rule, the experiment involves large focal volume averaging effects that act to reduce the ef-

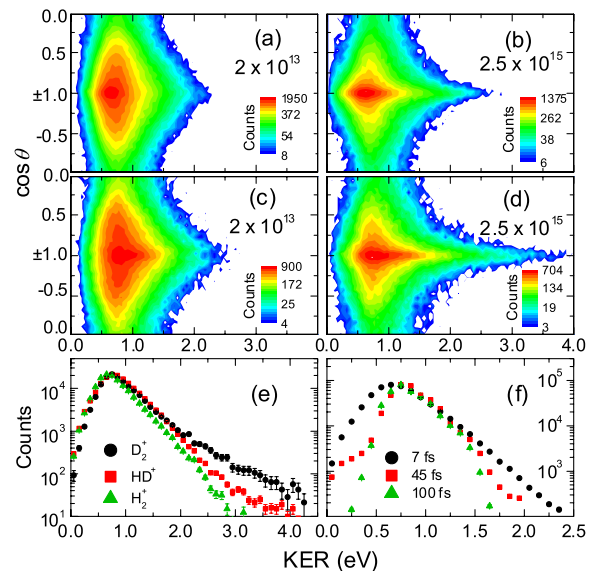


FIG. 3 (color online). (a),(b) Measured KER- $\cos\theta$ distributions for dissociation of H_2^+ using 7 fs pulses at intensities shown (in units of W/cm²). (c),(d) Same as (a),(b) for D_2^+ . (e) Total dissociation yield as a function of KER for H_2^+ , HD^+ , and D_2^+ at 7.5×10^{15} W/cm² normalized to the peak number of counts. (f) Same as (e) for H_2^+ at different pulse durations of 7, 45, and 100 fs at similar peak intensity (6.5 – 8.6×10^{14} W/cm²).

fective intensity—the reason for the small ionization fraction at 2.5×10^{15} W/cm². These are not accounted for in our theory. For these reasons, experiment and theory should be compared only qualitatively.

At low intensity, the distributions observed for H₂⁺ and D₂⁺ are quite similar. This agrees with our theory [Fig. 2(a)] which indicates that dissociation is predominantly one photon, and hence we do not expect there to be a strong isotopic dependence. At higher intensity, this is not the case. Experiment and theory reveal similar distributions for H₂⁺ despite the large difference in intensity, supporting our assertion of a lower overall effective intensity for the experiment. Most importantly, the signature high-KER tail is clearly observed. Moreover, it extends to almost the same maximum KER (~ 2.7 eV) as our theoretical prediction suggesting that it could similarly be a mixture of ATD₁ and ATD₂.

Comparison of H₂⁺ to D₂⁺ shows that this tail gets amplified and reaches much higher KER (~ 4.0 eV) for the more massive species. Recalling that ATD₂ was predicted to be suppressed and ATD₁ enhanced for D₂⁺ [Fig. 2(d)], the high-KER enhancement is likely from three- (or more) photon ATD₁. This is also in agreement with our channel-closing argument. The mass dependence is elucidated in Fig. 3(e) which shows the signal, integrated across all angles, for all three isotopologues at an intensity of 7.5×10^{15} W/cm². While the low-energy parts are similar, the high-energy portions display a progressive increase in KER with increasing mass.

As a final test to show explicitly the temporal dependence of ATD, we increased the pulse duration from 7 to 100 fs for H₂⁺ while maintaining approximately the same peak intensity, Fig. 3(f). The high-energy part of the spectrum clearly becomes enhanced for shorter pulse duration in agreement with the rest of our observations. Rather intriguingly, the low-energy part (< 0.5 eV) is also enhanced showing a strong pulse-length dependence.

Another mechanism that, in principle, can explain the high KER we have seen is a five-photon transition following the adiabatic pathway to $2p\sigma_u - 3\omega$. We believe this decay mechanism to be unlikely, however, because it requires a higher intensity than the three-photon transition. In addition, our calculation at 10^{14} W/cm² shows that the dominant contribution to the high KER observed comes from the vibrational states around the three-photon crossing with $1s\sigma_g$, and not the five-photon crossing [see Fig. 1(a)]. Nevertheless, we cannot rule out the possibility of at least weak five-photon contributions. There are a number of ways to experimentally test our argument. For example, laser pulse shaping could be used to produce a rapidly falling pulse to favor channel closing without affecting the five-photon ATD rate. Alternatively, selecting a specific initial vibrational state would allow the different

mechanisms to be separated much more cleanly, just as they were in our theory.

In summary, we have presented detailed evidence—combining state-of-the-art experimental and theoretical techniques—for our successful enhancement of high-order ATD using primarily the pulse length to control the dissociation pathways. In the course of this work, we also uncovered evidence not only of excited H(2I) contributions to dissociation but also of ATD through these states. The role of excited states has largely been ignored, but this Letter shows that their contributions at high KER should not be neglected.

The authors wish to thank Dr. C. Fehrenbach for his invaluable help in carrying out the experiments. This work was supported by the Chemical Sciences, Geosciences, and Biosciences Division, Office of Basic Energy Sciences, Office of Science, U.S. Department of Energy.

-
- [1] H. Stapelfelt and T. Seideman, *Rev. Mod. Phys.* **75**, 543 (2003).
 - [2] A. Hishikawa, A. Iwamae, and K. Yamanouchi, *Phys. Rev. Lett.* **83**, 1127 (1999).
 - [3] A. McPherson *et al.*, *J. Opt. Soc. Am. B* **4**, 595 (1987).
 - [4] A. H. Zewail, *J. Phys. Chem. A* **104**, 5660 (2000).
 - [5] T. Brixner *et al.*, *Phys. Rev. Lett.* **92**, 208301 (2004).
 - [6] B. D. Esry *et al.*, *Phys. Rev. Lett.* **97**, 013003 (2006).
 - [7] A. Staudte *et al.*, *Phys. Rev. Lett.* **98**, 073003 (2007).
 - [8] P. Agostini *et al.*, *Phys. Rev. Lett.* **42**, 1127 (1979).
 - [9] A. Giusti-Suzor *et al.*, *Phys. Rev. Lett.* **64**, 515 (1990).
 - [10] G. Jolicard and O. Atabek, *Phys. Rev. A* **46**, 5845 (1992).
 - [11] P. H. Bucksbaum *et al.*, *Phys. Rev. Lett.* **64**, 1883 (1990).
 - [12] A. Zavriyev *et al.*, *Phys. Rev. A* **42**, 5500 (1990).
 - [13] B. Yang *et al.*, *Phys. Rev. A* **44**, R1458 (1991).
 - [14] P. A. Orr *et al.*, *Phys. Rev. Lett.* **98**, 163001 (2007).
 - [15] A. Giusti-Suzor *et al.*, *J. Phys. B* **28**, 309 (1995).
 - [16] T. T. Nguyen-Dang *et al.*, *Phys. Rev. A* **67**, 013405 (2003).
 - [17] A. Talebpour *et al.*, *Phys. Rev. A* **62**, 042708 (2000).
 - [18] K. Vijayalakshmi *et al.*, *Phys. Rev. A* **62**, 053408 (2000).
 - [19] G. N. Gibson, L. Fang, and B. Moser, *Phys. Rev. A* **74**, 041401(R) (2006).
 - [20] F. Anis and B. D. Esry, *Phys. Rev. A* **77**, 033416 (2008).
 - [21] P. Q. Wang *et al.*, *Phys. Rev. A* **74**, 043411 (2006).
 - [22] E. Charron, A. Giusti-Suzor, and F. H. Mies, *Phys. Rev. A* **49**, R641 (1994).
 - [23] I. D. Williams *et al.*, *J. Phys. B* **33**, 2743 (2000).
 - [24] K. Sändig, H. Figger, and T. Hänsch, *Phys. Rev. Lett.* **85**, 4876 (2000).
 - [25] I. Ben-Itzhak *et al.*, *Phys. Rev. Lett.* **95**, 073002 (2005).
 - [26] X. M. Tong, Z. X. Zhao, and C. D. Lin, *Phys. Rev. Lett.* **91**, 233203 (2003).
 - [27] H. Mashiko *et al.*, *Appl. Phys. Lett.* **90**, 161114 (2007).
 - [28] P. Hansch, M. A. Walker, and L. D. VanWoerkom, *Phys. Rev. A* **54**, R2559 (1996).